Multifunctional Free-Standing Single-Walled Carbon Nanotube Films

Albert G. Nasibulin,[†,*] Antti Kaskela,[†] Kimmo Mustonen,[†] Anton S. Anisimov,[†] Virginia Ruiz,[†,‡] Samuli Kivistö,[§] Simas Rackauskas,[†] Marina Y. Timmermans,[†] Marko Pudas,[⊥] Brad Aitchison,[∥] Marko Kauppinen,[⊥] David P. Brown,[∥] Oleg G. Okhotnikov,[§] and Esko I. Kauppinen[†,*]

[†]Department of Applied Physics and Centre for New Materials, Aalto University, P.O. Box 15100, FI-00076 Aalto, Espoo, Finland, [‡]CIDETEC-IK4, P[o] Miramón 196, E-20009 Donostia-San Sebastián, Spain, [§]Optoelectronics Research Centre, Tampere University of Technology, P.O. Box 692, 33101 Tampere, Finland, [⊥]Microelectronics and Materials Physics Laboratories, EMPART Group, Infotech Oulu, University of Oulu, P.O. Box 4500, 90014 Oulu, Finland, and [∥]Canatu Ltd., Konalankuja 5, 00390 Helsinki, Finland

ABSTRACT We report a simple and rapid method to prepare multifunctional free-standing single-walled carbon nanotube (SWCNT) films with variable thicknesses ranging from a submonolayer to a few micrometers having outstanding properties for a broad range of exceptionally performing devices. We have fabricated state-of-the-art key components from the same single component multifunctional SWCNT material for several high-impact application areas: high efficiency nanoparticle filters with a figure of merit of 147 Pa^{-1}, transparent and conductive electrodes with a sheet resistance of 84 Ω/□ and a transmittance of 90%, electrochemical sensors with extremely low detection limits below 100 nM, and polymer-free saturable absorbers for ultrafast femtosecond lasers. Furthermore, the films are demonstrated as the main components in gas flowmeters, gas heaters, and transparent thermoacoustic loudspeakers.

KEYWORDS: aerosol filter · transparent and conductive electrodes · electrochemical sensors · saturable absorbers · applications

The unique properties of single-walled carbon nanotube (SWCNT) films, such as high porosity and specific surface area, low density, high ratio of optical transmittance to sheet resistance, high thermal conductivity and chemical sensitivity, and tunable metallic and semiconducting properties, open up a new avenue for a wide range of applications.[1] Free-standing films (FSFs) offer a unique form factor for novel applications. Films of randomly oriented SWCNTs are usually prepared from suspensions by vacuum-filtration method.[2,3] This method typically involves several time- and resource-consuming and potentially detrimental liquid dispersion and purification steps ending up with dense SWCNT networks on a filter,[4,5] which are difficult to transfer issue. Moreover, preparation of free-standing films by the vacuum-filtration method is still a challenging task.

Here, we have developed an aerosol CVD synthesis method[6,7] for direct deposition of SWCNT, which eliminates all mentioned problems. The films are prepared by first collecting nanotubes downstream of the reactor on microporous filters (Millipore, HAWP, 0.45 μm pore diameter) and then dry transferring them to a substrate with an opening as shown in Figure 1 (see also the Supporting Information),[8] thus demonstrating a very simple and rapid fabrication technique. The thickness of the SWCNT films can be varied from a submonolayer (when the amount of SWCNTs is insufficient to create a single continuous layer) to a few micrometers depending on the collection time. Since the SWCNT films are collected on low-adhesion filters, they can be easily transferred to practically any substrate, including flexible polymers, glass, quartz, silicon, and various metals. In this work, we have successfully fabricated FSFs up to 70 mm in diameter, which can be easily further scaled up. For some applications, the FSFs can be densified by drop-casting with ethanol and subsequent drying in air (see Supporting Information). This results in a change in the surface roughness and therefore reflectance of the SWCNT films, as can be visually observed in Figure 1.

RESULTS AND DISCUSSION

Due to the fact that the SWCNT films have very high porosity, the FSFs were found to be exceptionally good air filters. In order to examine the filter performance, we used various sources of aerosol particles with geometric mean diameters in the range of 11 to 650 nm (see Supporting Information). Figure 2a shows the number size distribution of 11 nm Fe aerosol particles produced by a hot-wire particle generator and the drop in the aerosol particle concentration after passing through a 70 nm thick SWCNT filter. The filter efficiency was calculated as

$$E = \frac{C_{in} - C_{out}}{C_{in}} \times 100\%$$

* Address correspondence to albert.nasibulin@hut.fi, esko.kauppinen@hut.fi.

Received for review January 26, 2011 and accepted March 1, 2011.

Published online March 01, 2011
10.1021/nn200338r

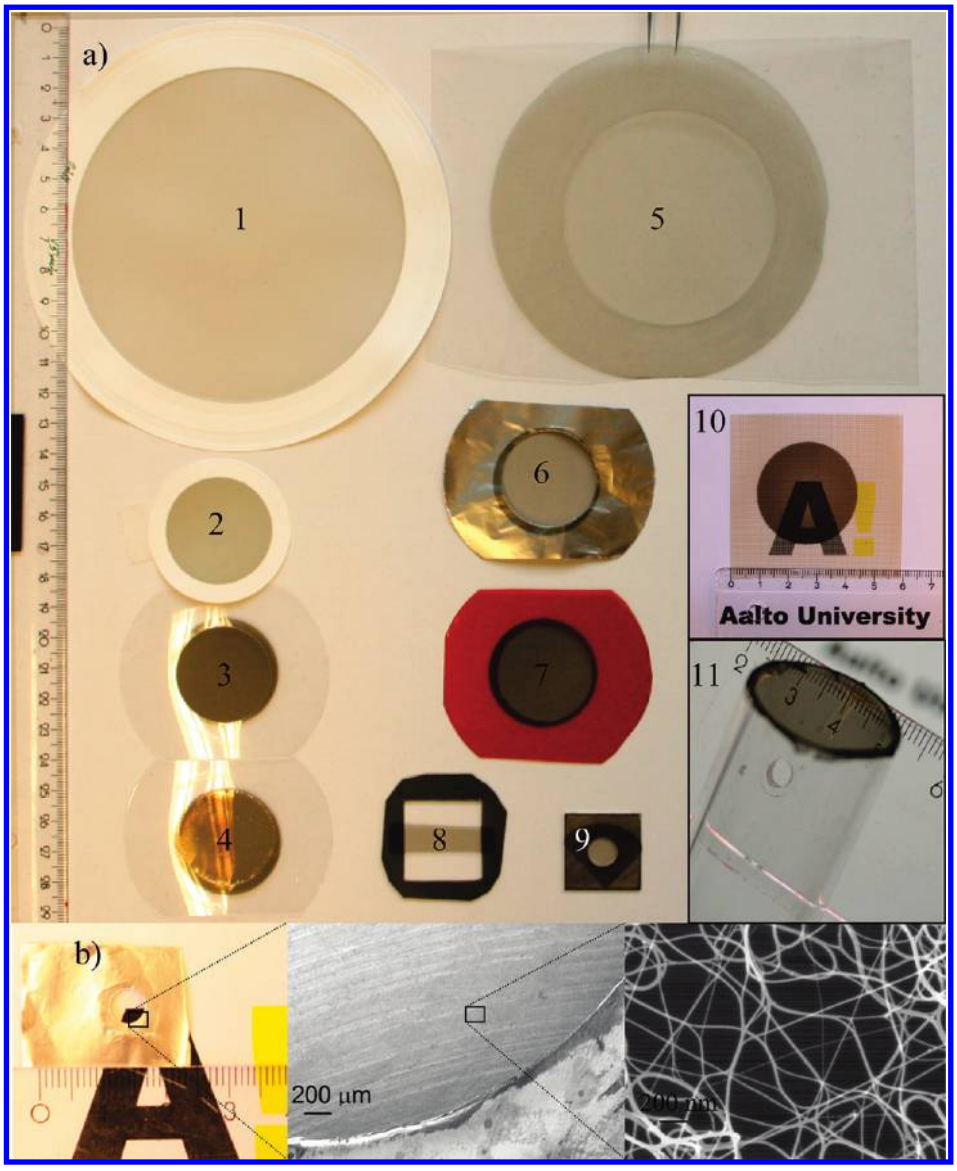

Figure 1. (a) Photograph of nitrocellulose filters with collected SWCNT films (1,2), pristine and ethanol-densified films suspended over 30 mm openings in PET (3 and 4, respectively), FSF on PET over 70 mm hole (5), FSF on aluminum foil (6), FSF on Kapton (7), a strip of FSF suspended over a rectangular hole in a plastic sheet (8), and FSF on cold rolled steel (9). The inset shows (10) a semi-free-standing film on a polyetheretherketone substrate with 120 μm diameter holes (with an open area of 49%) and (11) an FSF suspended over the open end of a glass tube of internal diameter 20 mm. (b) Set of images showing a submonolayer FSF suspended over 5 mm openings in aluminum foil.

where C_{in} and C_{out} are the aerosol concentrations measured with and without the filter, respectively. Figure 2b shows the dependence of the filter collection efficiency on the SWCNT film thickness for 44 nm γ-Fe_2O_3 particles. The efficiency of the filter increases from 99.995 to 99.9997% as the film thickness increases from 40 to 200 nm.

Another very important filter characteristic is the pressure drop. This was measured as a function of the flow rate through a 120 nm thick SWCNT film suspended over a 1 cm hole (Figure 2c). For comparison, we utilized several different commercially available filters (Millipore). Figure 2c shows that the SWCNT filters create significantly smaller pressure drops than do the others tested. The absolute quality of a particle filter is usually evaluated on the basis of its collection efficiency for a given particle size and pressure drop Δp from the following formula:[9]

$$q_F = -\frac{\ln(1-E)}{\Delta p}$$

As can be seen from Figure 2d, the quality factor q_F of the SWCNT films is at least an order of magnitude higher than that of the commercially available filters and reaches a maximum value of 147 Pa^{-1}.

The filtration efficiency for aerosolized SWCNTs was greater than 99.999%. When the FSFs were used for filtration of SWCNTs at the outlet of a laboratory-scale

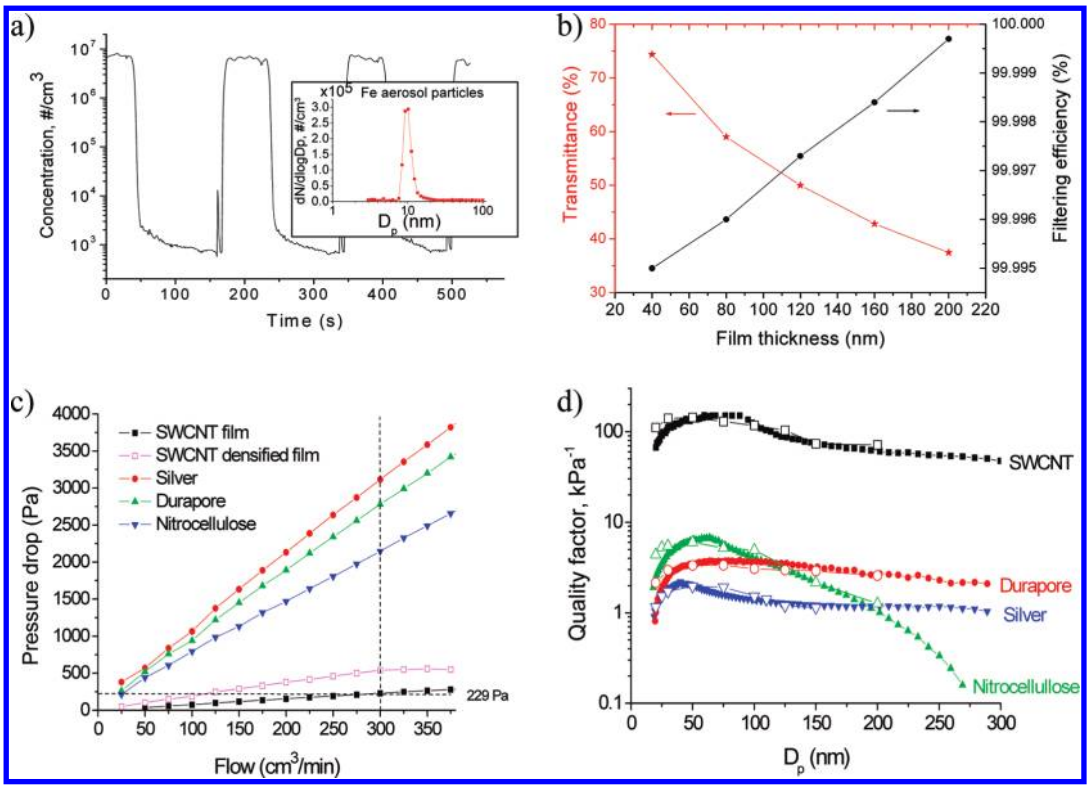

Figure 2. FSF air filter characterization. (a) Change in 11 nm sized Fe particle concentration measured by a particle counter when the flow passed alternately through a filter and a bypass. The film is 70 nm thick with transmittance of 64% and filtering efficiency of 99.99% The inset shows the number size distribution of the Fe particles used for the efficiency test. (b) Thickness dependence of transmittance and of collection efficiency for 44 nm γ-Fe_2O_3 particles. (c) Flow rate dependence of pressure drop for 120 nm thick SWCNT films and various commercial filters. (d) Dependence of the filter quality factor on the particle size for commercial filters and a 120 nm thick SWCNT film. The solid and open symbols show results obtained by two independent measurement techniques, namely, scanning over the entire particle size range studied and at fixed particle sizes.

aerosol reactor, the SWCNT concentration dropped from above 10^7 particles/cm^3 to a noise level of less than 1 particle/cm^3. Interestingly, when a hole of about 1 mm diameter was made in the FSF, it self-healed in about 5 min owing to the deposition of SWCNTs at the edges.

In spite of their thinness, the FSFs were surprisingly strong and durable. To investigate the maximum pressure and flow rate which the filters could withstand before breakage, we suspended SWCNT filters over a hole 1 cm in diameter. It was found that a 40 nm thick film could withstand a flow of 1.7 L/min, with a corresponding flow velocity of 36 cm/s and a pressure drop of 480 Pa (see Supporting Information). Durability tests performed with a similar filter showed that the filter was able to operate for more than a month without breakage or reduction in the filtration efficiency at a flow rate of 300 cm^3/min.

The mechanical strength of such films was measured using a perforation method in which the films were pressed against a 1.5 mm ball-shaped actuator (see Supporting Information). The force *versus* displacement was used as a measure of a film-stiffness-like property in the linear region (Figure 3a). It is worth noting that the FSFs were neither purely elastic nor purely viscoelastic. In fact, for very small deformations, the film responds elastically, but when the deformation is continued, it begins to behave viscoelastically. Similar behavior was earlier reported by Zhu *et al.* for SWCNT strands.[10] The slope of the linear fits shown in Figure 3a represents the stiffness-like property of the films and was found to increase with the film thickness. Moreover, the maximum force required to partially damage the film (dashed lines) also increased with the film thickness. From the maximum force needed for the first breakage, we calculated the ultimate tensile strength to be 65−115 MPa. These values are at the same level as or higher than the ultimate strength of common polymers, for example, high-density polyethylene (37 MPa) and nylon-6,6 (75 MPa).

The high transmittance and electrical conductivity of SWCNT films enable their use as a replacement for indium−tin oxide (ITO), especially in applications where ITO is not suitable owing to high cost, performance limitations, or environmental impact. Figure 3b shows the dependence of sheet resistance on optical transparency (at 550 nm) for ethanol-densified and NO_2-doped SWCNT films. For comparison, data for commercially available ITO films on flexible substrates and for other carbon nanotube (including double-walled carbon nanotube, DWCNT) films[8,11,12] are shown in the figure, as well. The NO_2-doped SWCNT films exhibited

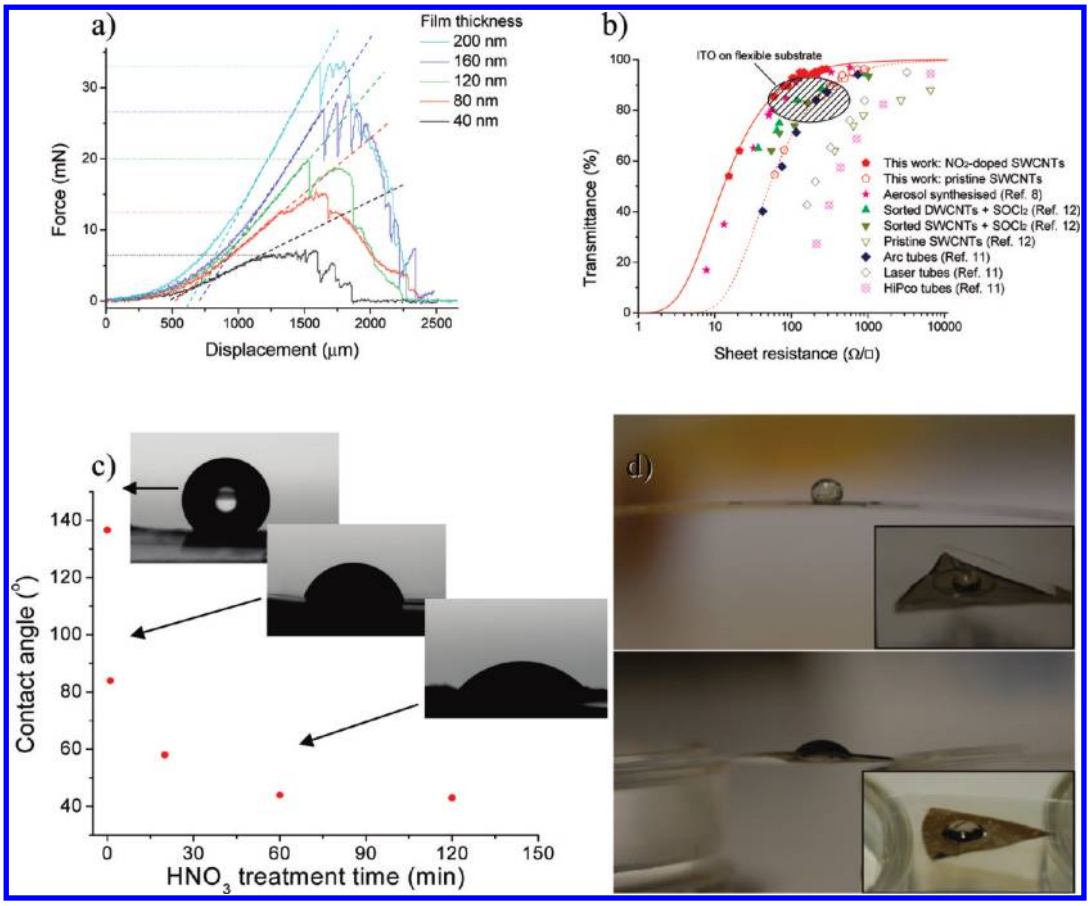

Figure 3. Properties of FSFs. (a) Results of mechanical tests on pristine films of different thicknesses. The film stiffness was determined from the slope of linear fits. (b) Comparison of different transparent electrode materials: sheet resistance *versus* optical transparency at 550 nm. Our data are shown by open pentagons (densified films) and solid pentagons (NO_2-doped films); the lines show theoretical fits to our data.[8] The performance range of commercially available ITO films on PET (Visiontek Systems Ltd., UK) is shown by the oval. (c,d) Alteration of hydrophobic properties by acid treatment of (c) SWCNTs on silica and (d) SWCNTs suspended over a hole. FSFs are shown before and after HNO_3 treatment holding a droplet of water with a weight of 3000 times their own weight. After the acid treatment, the droplet penetrated through the SWCNT film and fully wetted the film from top and bottom.

sheet resistances as low as 84 Ω/□ at a transmission of $T = 90\%$. This is superior to the typical performance of ITO on flexible polymer substrates and, to our knowledge, is the lowest reported sheet resistance for SWCNT-based transparent electrodes. Importantly, our method avoids liquid-based dispersion and purification steps, which are needed with traditional SWCNT film production techniques. Moreover, our SWCNT films can be utilized equally well in free-standing form or on virtually any substrate, including flexible polyethylene terephthalate (PET) and naphthalate (PEN). We obtained very similar optical and electrical behavior for free-standing and substrate-supported films.

SWCNT electrodes can be successfully utilized in electroanalysis. Owing to their unique properties such as high conductivity and surface area, electrochemical stability, low background currents, and electrocatalytic properties in many electrochemical reactions, SWCNTs have been extensively used for electrochemical sensing.[13] There are many strategies for integrating SWCNTs into electrochemical sensors, the main ones being direct growth on insulating or conducting supports and immobilization of the SWCNTs on the electrode surface with the aid of binders and dispersing agents.[14] Here we show the excellent sensing properties of our FSF electrodes for the electrochemical detection of dopamine, a neurotransmitter often taken as a benchmark analyte for investigating the sensing properties of electrode materials. Figure 4a shows cyclic voltammograms of an FSF electrode (60% transmittance at 550 nm) for dopamine oxidation in a 0.1 M phosphate buffer solution (PBS) with pH = 7. The voltammetry for the dopamine/dopamine *o*-quinone reaction exhibited quasi-reversible behavior ($\Delta E_p \approx 90$ mV at low dopamine concentrations). The peak current scales linearly with dopamine concentration, as shown in the inset of the figure, over a wide concentration range (from 0.1 to 100 μM, $R^2 = 0.994$). Despite its thinness (about 80 nm), the FSF electrode shows a remarkable sensitivity (253 $\mu A\ mM^{-1}\ cm^{-2}$), as determined from the slope of the linear regression.

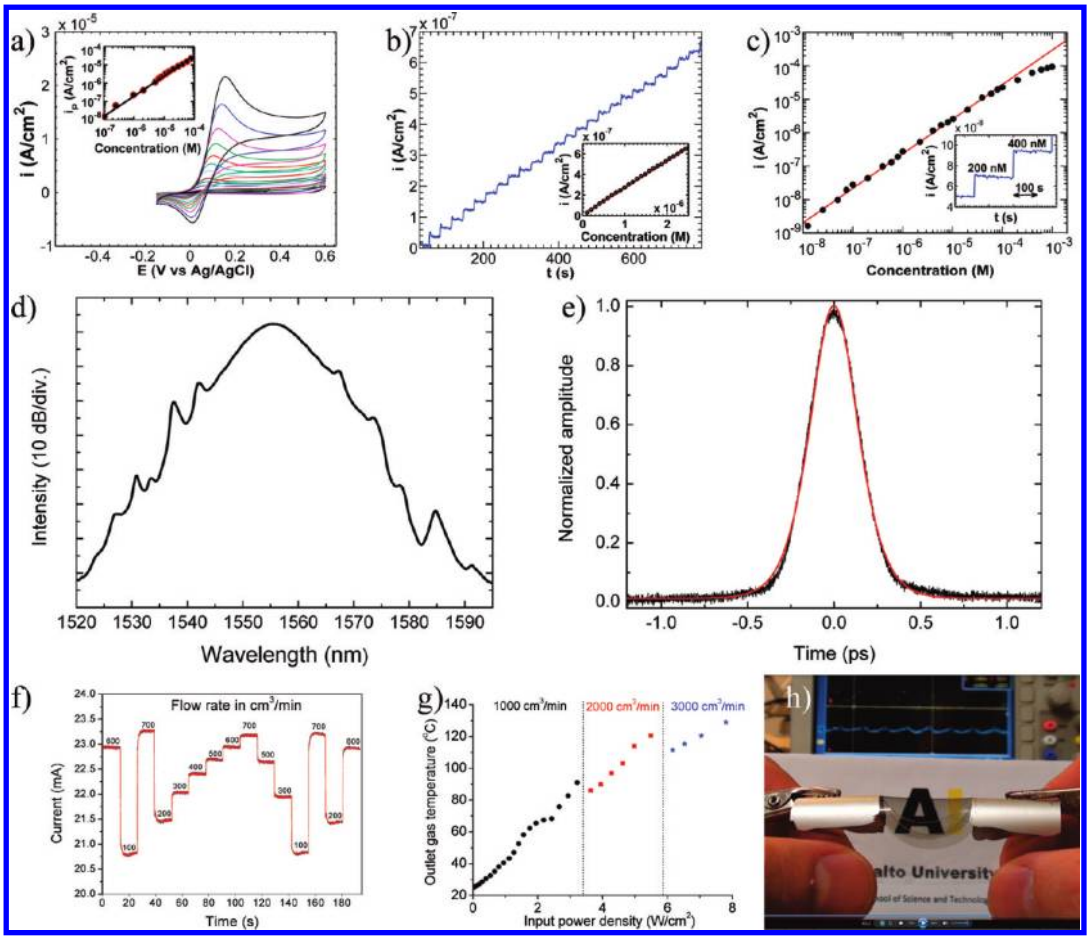

Figure 4. FSFs for various applications. (a−c) Chemical sensor. (a) Cyclic voltammograms of an FSF electrode in solutions with increasing concentrations of dopamine (from 0.1 to 80 μM). Scan rate: 50 mV s^{-1}. The inset shows the peak current *versus* dopamine concentration and the corresponding linear fit. (b) Amperometric response of an FSF electrode to successive additions of 100 nM dopamine at an applied potential of +0.2 V *versus* Ag/AgCl. The inset shows the corresponding calibration plot. (c) Calibration plot for the amperometric response of an FSF electrode at an applied potential of +0.2 V *versus* Ag/AgCl in solutions with increasing dopamine concentration. The inset shows the stability of the SWCNT sensor at the operating potential at very low dopamine concentrations. The supporting electrolyte was a 0.1 M PBS with pH = 7. (d,e) Laser absorber: (d) optical spectrum and (e) autocorrelation trace with a sech^2 fit for an all-fiber mode-locked Er laser. The spectral width is ∼11.3 nm and the corresponding pulse width is 220 fs. (f) Gas flowmeter. Electrical current through the FSF at different nitrogen flow rates. (g) Gas heater. Temperature of outflowing gas *versus* input power density at different flow rates. (h) Thermoacoustic speaker based on SWCNTs. Demonstration of its flexibility.

The operating potential for the amperometric detection of dopamine was selected from a hydrodynamic voltammogram measured in 0.1 mM dopamine. Figure 4b shows a close-up of the low-concentration region of the amperometric response of FSF sensor (with a 60% transmittance) at +0.2 V (*versus* Ag/AgCl), measured with successive additions of 100 nM dopamine in a stirred solution. The corresponding calibration plot, shown in the inset, illustrates the remarkable linearity exhibited by the FSF sensor in this low concentration range (0.1−3 μM, R^2 = 0.999), with a sensitivity of 263 μA mM^{-1} cm^{-2}. Extremely low detection limits, in the nanomolar range (100 nM), were achieved. This performance is comparable to that reported for low-density SWCNT networks on Si/SiO$_2$ wafers.[15] The sensor also exhibits a very fast response time of 2−3 s. In addition to the excellent behavior at concentrations in the nanomolar range, the FSF sensor exhibits a good linear response (R^2 = 0.995) over a wide concentration range (0.01 μM to 0.1 mM) (Figure 4c) while retaining a remarkable sensitivity (240 μA mM^{-1} cm^{-2}) and detection limits in the nanomolar range. Moreover, the inset in Figure 4c demonstrates the high stability of the amperometric response of the SWCNT sensor for very low concentrations at the operating potential (+0.2 V *versus* Ag/AgCl). To the best of our knowledge, linear ranges over 4 orders of magnitude of dopamine concentration together with nanomolar detection limits are unprecedented for untreated SWCNT-based macroelectrodes. The high sensitivity, stability, and reproducibility for dopamine detection shown by the unmodified FSF electrodes demonstrate the potential of this type of pristine unsupported film for electroanalysis.

Another important application for FSFs is a laser component, namely, a saturable absorber for ultrafast

photonics. A key element in the cavity of a mode-locked fiber laser is the nonlinear element that initiates the pulsed operation. SWCNTs have been demonstrated recently to initiate short pulses in mode-locked fiber and solid-state lasers.[16−20] These mode-lockers benefit from a fairly simple and cost-effective manufacturing process, a broad absorption band, and a short absorption recovery time. Typically, carbon nanotubes have been embedded into a polymer.[16,18−20] Polymers are often undesirable as intracavity laser materials owing to their relatively low damage threshold and high photoabsorption, especially for mid-infrared applications. In the present work, we have demonstrated the use of an FSF to mode-lock a compact ultrafast erbium-doped fiber laser operating at a wavelength of 1.56 μm. This absorber, made purely of carbon nanotubes, benefits from a very simple and fast manufacturing process. Time-consuming wet deposition methods, which require several processing stages and include matrix polymers, are not needed. Moreover, the FSFs can be used as a mode-locker "as-deposited" without any bulk components (*i.e.*, mirrors or other substrates).

The mode-locked fiber laser delivered pulses with a repetition rate of 38.3 MHz. The recorded optical pulse spectrum and corresponding autocorrelation trace are shown in Figure 4d,e. The Kelly side bands seen in the spectrum confirm operation in the soliton pulse regime. A hyperbolic-secant (sech^2) fit of the measured autocorrelation revealed a short pulse duration of 220 fs. The pulses at the output are transform-limited, with a calculated time−bandwidth product of ~0.32. To the best of our knowledge, this is the first demonstration of the use of an SWCNT-based saturable absorber for mode-locking without any substrate.

These FSFs are an interesting material for certain types of applications where low heat capacity and high thermal conductivity are required. As an example, we have constructed a thermal flow sensor with a working principle similar to that of a hot-wire gas flowmeter:[21] the flow passes through a resistively heated FSF, and its temperature changes until dynamic thermal equilibrium is achieved. As a result, the resistivity of the film is changed. An example of the long-term performance and stability of such a flowmeter in nitrogen at different flow rates is shown in Figure 4f. Depending on the flow rate, the flowmeter provides response times in the range of 20−100 ms (see Supporting Information).

By combining the electrical heating and gas penetration properties, our FSFs can be utilized as efficient gas heaters. Usually, heater elements operate at relatively high temperatures since the contact between the gas and the heater is limited. However, owing to the high surface area of the FSFs, the contact can be significantly improved. It was found that a 80 nm thick FSF suspended over an opening with an area of 1.05 cm^2 in a PET substrate was able to heat a 3 L/min nitrogen flow to 129 °C as measured with a thermocouple after the film (see Supporting Information). This corresponds to a heat power density of 8 W/cm^2 (Figure 4g). Similar measurements in air allowed the flow to be heated to 90 °C with a power density of about 3 W/cm^2.

The first thermoacoustic speaker based on carbon nanomaterials was introduced by Xiao *et al.*[22] These authors fabricated loudspeaker elements from free-standing sheets of aligned multiwall carbon nanotubes (MWCNTs) prepared by drawing from a substrate consisting of a CVD-grown MWCNT forest.[23] Xiao *et al.* also claimed that SWCNT networks could be used as loudspeakers, but that the fabrication of elements from free-standing SWCNT networks would be extremely tedious. Here, for the first time, we have demonstrated thermoacoustic speakers using FSFs made from randomly oriented SWCNTs (Figure 4h; see also Supporting Information).

Carbon nanotubes are known to possess hydrophobic properties, which limits many of their potential applications. During HNO_3 treatment of SWCNT films, it was found that the water wettability of the SWCNTs can be changed from nearly superhydrophobic to hydrophilic (Figure 3c,d). This opens up new avenues for applications of SWCNT films, for instance, for water purification and filtration. In this case, the filtration could be realized using semi-free-standing films, where the SWCNTs are transferred onto a polymer with micrometer or millimeter-sized holes (Figure 1).

The wide range of applications of these FSFs is not limited to those reported in this article. The superior mechanical and electrical properties of these films suggest potential uses in a broad range of other devices. As a filter, SWCNT films could be used for filtration of bacteria and even viruses, whose size (10−60 nm) is exactly in the range where our film filters showed excellent performance. The possibility to heat SWCNT films can be utilized for water or air sterilization. Additionally, since SWCNTs contain iron particles embedded inside them, one could exploit their magnetic properties. Their high strength coupled with high electrical conductivity could be employed in novel energy generators, electromagnetic interference shielding, flexible radio frequency identification tags, touch sensors, flat panel displays, and static-charge dissipators. The ultrahigh surface area coupled with high electrical conductivity could be used in advanced solar cells and supercapacitors. It is very important to note here that these multifunctional films also have many application opportunities in their non-free-standing, that is, substrate-supported, state as well.[24,25] The outstanding combination of mechanical, electrical, and optical properties of our SWCNTs enables a wide range of superior functionality to be obtained from FSFs made from them. Even though graphene has recently attracted much attention from the research community, some properties of SWCNTs, such as

porosity, mechanical strength, and fine-tunability of optical and electrical properties, provide many applications where the flat, single-layered carbon structure cannot compete with its tubular "brother".

CONCLUSIONS

We have reported a simple method for the rapid fabrication of multifunctional thin FSFs, which can be utilized in various applications. Here, we have demonstrated the use of these FSFs for exceptionally efficient air filtration and very sensitive electrochemical sensing, and as substrate-free laser absorbers and as state-of-the-art transparent electrodes with properties better than ITO on a flexible substrate. Furthermore, these FSFs have been utilized as the main components in a gas flowmeter, a heater, and thermoacoustic loudspeaker. Our multifunctional films open up possibilities both for basic scientific research on this unique material, that is, single-walled carbon nanotubes, and for a wide range of commercial applications, where lightweight, high surface area and porosity, high thermal and electrical conductivity, and optical transparency are desired.

METHODS

SWCNT Synthesis. SWCNTs were synthesized by an aerosol (floating catalyst) method based on ferrocene vapor decomposition in a CO atmosphere.[6] The catalyst precursor was vaporized by passing ambient temperature CO (at a flow rate of 300 cm^3/min) through a cartridge filled with ferrocene powder. The flow containing ferrocene vapor (at 0.7 Pa) was then introduced into the high-temperature zone of a ceramic tube reactor through a water-cooled probe and mixed with additional CO (100 cm^3/min). The reactor tube was 22 mm in diameter with a heating zone 470 mm long. Typically, the SWCNTs produced by this method were bundles with lengths from 1 to 5 μm and diameters in the range of 1.3−2.0 nm. The second experimental setup used for SWCNT synthesis was a scaled-up version of the laboratory reactor, with a tube 155 mm in diameter and 1500 mm in length to provide a longer residence time. It was operated at a total CO flow rate of 4 L/min and a temperature of 880 °C. This allowed us to synthesize SWCNT bundles about 10 μm long. In both reactors, to obtain stable growth of SWCNTs, a controlled amount of carbon dioxide was added together with the carbon source (CO).[26] SWCNTs were collected downstream of the reactor by filtering the flow through a nitrocellulose or silver membrane filter (Millipore Corp., USA; HAWP, 0.45 μm pore diameter).

Fabrication of Free-Standing Films. The simplicity and rapidity of the preparation of free-standing films (FSFs) of SWCNTs is demonstrated in Figure S1 and Movie 1 in Supporting Information. The SWCNTs, collected on a filter, can be easily transferred onto practically any substrate by a room temperature dry-press transfer technique.[8] Movie 1 shows a flexible polyethylene terephthalate (PET) substrate with a 30 mm hole pressed against a filter with collected SWCNTs fixed on a table. The applied pressure provides conformal contact, and the SWCNT network adheres to the substrate. After that, the polymer substrate can be removed by lifting. The transfer process is extremely simple, and no dispersion or cleaning steps are needed prior to press transfer. This makes the process significantly faster, cheaper, and more environmentally friendly than traditional liquid-based SWCNT network deposition processes. The size of the FSF can be increased at least up to 70 mm in diameter (Figure 1).

The scaled-up aerosol reactor was operated under conditions in which 1 min of SWCNT collection on a filter with a diameter of 5 cm resulted in a 40 nm thick SWCNT film (after densification). The deposition rate was measured by means of transmission electron microscopy for 1−5 min SWCNT collections. For this purpose, SWNTs were first densified and embedded in an epoxy polymer. Then, 50 nm thick cross sections of epoxy layers carrying SWCNT films were cut and deposited directly on TEM grids. Figure S2a presents TEM images of a sandwich structure consisting of a 120 nm thick SWCNT film (collected during 3 min) between epoxy layers. The thicknesses of SWCNTs were estimated on the basis of calibration dependence of transmittance *versus* thickness (Figure 2b).

Acknowledgment. The authors thank Prof. S.-G. Sjölind for calculations of mechanical properties, and A. Nykänen, R. Tommila, Dr. J. Raula, L. I. Nasibulina, and B. F. Mikladal for their assistance during experiments. T. Murto and J. Sarkkinen are gratefully acknowledged for their help in the sample preparation. The authors thank Prof. F. Banhart for high-resolution TEM imaging. This work was supported by the Academy of Finland (Project Numbers 128445, 128495, and 130533), TEKES (Project Numbers 40371/06 and 402701/08), and Aalto University through the Multidisciplinary Institute of Digitalization and Energy (CNB-E project) programme, and by the Spanish Ministry of Science and Innovation (Programme Ramón y Cajal).

Supporting Information Available: Fabrication of free-standing films (movie 1), postsynthesis treatment of free-standing films (movie 2), particle generation for filter efficiency experiments and aerosol measurements, mechanical tests on free-standing SWCNT films, laser mode-locking and experimental setup, electrochemical sensing, flowmeter (movie 3), gas heater, thermoacoustic speaker (movie 4). This material is available free of charge *via* the Internet at http://pubs.acs.org.

REFERENCES AND NOTES

1. Saito, R.; Dresslhaus, G.; Dresselhaus, M. S. *Physical Properties of Carbon Nanotubes*; Imperial College Press: London, 1996; p 258.
2. Gu, H.; Swager, T. M. Fabrication of Free-Standing, Conductive, and Transparent Carbon Nanotube Films. *Adv. Mater.* **2008,** *20*, 4433–4437.
3. Aldeanueva-Potel, P.; Correa-Duarte, M. A.; Alvarez-Puebla, R. A.; Liz-Marzán, L. M. Free-Standing Carbon Nanotube Films as Optical Accumulators for Multiplex SERRS Attomolar Detection. *ACS Appl. Mater. Interfaces* **2010,** *2*, 19–22.
4. Zhou, Y.; Hu, L.; Gruner, G. A Method of Printing Carbon Nanotube Thin Films. *Appl. Phys. Lett.* **2006,** *88*, 123109.
5. Lim, C.; Min, D.-H.; Lee, S.-B. Direct Patterning of Carbon Nanotube Network Devices by Selective Vacuum Filtration. *Appl. Phys. Lett.* **2007,** *91*, 243117.
6. Moisala, A.; Nasibulin, A. G.; Brown, D. P.; Jiang, H.; Khriachtchev, L.; Kauppinen, E. I. Single-Walled Carbon Nanotube Synthesis Using Ferrocene and Iron Pentacarbonyl in a Laminar Flow Reactor. *Chem. Eng. Sci.* **2006,** *61*, 4393–4402.
7. Nasibulin, A. G.; Pikhitsa, P. V.; Jiang, H.; Brown, D. P.; Krasheninnikov, A. V.; Anisimov, A. S.; Queipo, P.; Moisala, A.; Gonzalez, D.; Lientschnig, G.; *et al.*A Novel Hybrid Carbon Material. *Nat. Nanotechnol.* **2007,** *2*, 156–161.
8. Kaskela, A.; Nasibulin, A. G.; Zavodchikova, M. Y.; Aitchison, B.; Papadimitratos, A.; Tian, Y.; Zhu, Z.; Jiang, H.; Brown, D. P.; Zakhidov, A.; *et al.*Aerosol Synthesized SWCNT Networks with Tuneable Conductivity and Transparency by Dry Transfer Technique. *Nano Lett.* **2010,** *10*, 4349–4355.
9. Hinds, W. C. *Aerosol Technology: Properties, Behavior, And Measurement of Airborne Particles*; Wiley-Interscience: New York, 1999; p 504.

10. Zhu, H. W.; Xu, C. L.; Wu, D. H.; Wei, B. Q.; Vajtai, R.; Ajayan, P. M. Direct Synthesis of Long Single-Walled Carbon Nanotube Strands. *Science* **2002,** *296*, 884–886.
11. Geng, H.-Z.; Lee, Y. H. Transparent Conducting Films by Using Carbon Nanotubes. In *Nanoscale Phenomena-Basic Science to Device Applications*; Tang, Z., Sheng, P., Eds.; Springer Publishers: Berlin, 2007; pp 15−28.
12. Green, A. A.; Hersam, M. C. Processing and Properties of Highly Enriched Double-Wall Carbon Nanotubes. *Nat. Nanotechnol.* **2009,** *4*, 64–70.
13. Gong, K.; Yan, Y.; Zhang, M.; Su, L.; Xiong, S.; Mao, L. Electrochemistry and Electroanalytical Applications of Carbon Nanotubes: A Review. *Anal. Sci.* **2005,** *21*, 1383–1393.
14. Merkoçi, A.; Pumera, M.; Llopis, X.; Pérez, B.; del Valle, M.; Alegret, S. New Materials for Electrochemical Sensing VI: Carbon Nanotubes. *Trends Anal. Chem.* **2005,** *24*, 826–838.
15. Bertoncello, P.; Edgeworth, J. P.; Macpherson, J. V.; Unwin, P. R. Trace Level Cyclic Voltammetry Facilitated by Single-Walled Carbon Nanotube Network Electrodes. *J. Am. Chem. Soc.* **2007,** *129*, 10982–10983.
16. Set, S. Y.; Yaguchi, H.; Tanaka, Y.; Jablonski, M. Laser Mode Locking Using a Saturable Absorber Incorporating Carbon Nanotubes. *J. Lightwave Technol.* **2004,** *22*, 51–56.
17. Kivisto, S.; Hakulinen, T.; Kaskela, A.; Aitchison, B.; Brown, D. P.; Nasibulin, A. G.; Kauppinen, E. I.; Harkonen, A.; Okhotnikov, O. G. Carbon Nanotube Films for Ultrafast Broadband Technology. *Opt. Express* **2009,** *17*, 2358–2363.
18. Cho, W. B.; Yim, J. H.; Choi, S. Y.; Lee, S.; Schmidt, A.; Steinmeyer, G.; Griebner, U.; Petrov, V.; Yeom, D. I.; Kim, K.; *et al.* Carbon Nanotubes: Boosting the Non Linear Optical Response of Carbon Nanotube Saturable Absorbers for Broadband Mode-Locking of Bulk Lasers. *Adv. Funct. Mater.* **2010**10.1002/adfm.201090048.
19. Hasan, T.; Sun, Z.; Wang, F.; Bonaccorso, F.; Tan, P. H.; Rozhin, A. G.; Ferrari, A. C. Nanotube−Polymer Composites for Ultrafast Photonics. *Adv. Mater.* **2009,** *21*, 3874–3899.
20. Schibli, T.; Minoshima, K.; Kataura, H.; Itoga, E.; Minami, N.; Kazaoui, S.; Miyashita, K.; Tokumoto, M.; Sakakibara, Y. Ultrashort Pulse-Generation by Saturable Absorber Mirrors Based on Polymer-Embedded Carbon Nanotubes. *Opt. Express* **2005,** *13*, 8025–8031.
21. Goldstein, R. J. *Fluid Mechanics Measurements*; Taylor & Francis: Washington DC, 1996; p 600.
22. Xiao, L.; Chen, Z.; Feng, C.; Liu, L.; Bai, Z.-Q.; Wang, Y.; Qian, L.; Zhang, Y.; Li, Q.; Jiang, K.; *et al.* Flexible, Stretchable, Transparent Carbon Nanotube Thin Film Loudspeakers. *Nano Lett.* **2008,** *8*, 4539–4545.
23. Zhang, M.; Fang, S.; Zakhidov, A. A.; Lee, S. B.; Aliev, A. E.; Williams, C. D.; Atkinson, K. R.; Baughman, R. H. Strong, Transparent, Multifunctional, Carbon Nanotube Sheets. *Science* **2005,** *309*, 1215–1219.
24. Cao, Q.; Rogers, J. A. Ultrathin Films of Single-Walled Carbon Nanotubes for Electronics and Sensors: A Review of Fundamental and Applied Aspects. *Adv. Mater.* **2009,** *21*, 29–53.
25. Hu, L.; Hecht, D. S.; Grüner, G. Carbon Nanotube Thin Films: Fabrication, Properties, and Applications. *Chem. Rev.* **2010,** *110*, 5790–844.
26. Nasibulin, A. G.; Brown, D. P.; Queipo, P.; Gonzalez, D.; Jiang, H.; Kauppinen, E. I. An Essential Role of CO_2 and H_2O during Single-Walled CNT Synthesis from Carbon Monoxide. *Chem. Phys. Lett.* **2006,** *417*, 179–184.